Journal of ELECTRONIC MATERIALS, Vol. 48, No. 3, 2019
https://doi.org/10.1007/s11664-018-06912-x

Optoelectronic Properties of a Simple Metal-Free Organic Sensitizer with Different Spacer Groups: Quantum Chemical Assessments

AMMASI ARUNKUMAR[1] and PONNUSAMY MUNUSAMY ANBARASAN[1,2]

1.—Department of Physics, Periyar University, Salem 636 011, India. 2.—e-mail: profpmanbarasan@gmail.com

The optimized geometries, electronic structures, absorption spectra and nonlinear optical (NLO) properties of five donor-π-spacer-acceptor (D-π-A)-based organic molecules, namely indolocarbazole-3,4-ethylenedioxythiophene, indolocarbazole-benzothiadiazole, indolocarbazole-furan, indolocarbazole-quinoxaline and indolocarbazole-benzoxadiazole (ICZS1–ICZS5), are analyzed using density functional theory (DFT) and time-dependent DFT (TD-DFT) methods. The performance of three functionals, Becke's three parameter Lee–Yang–Parr (B3LYP), Coulomb-attenuating method-B3LYP (CAM-B3LYP) and Grimme's D2 dispersion model (WB97XD), were analyzed for indolo[3,2,1-jk]carbazole (IC-2). The computed results indicated that absorption spectra of WB97XD are closest to IC-2. As a result, the WB97XD functional was chosen for further studies of ICZS1–ICZS5 dyes. The designed molecules also show excellent performance in terms of smaller energy gap, chemical hardness, red-shifted longer wavelength, free energy change for electron injection, dye regeneration and NLO properties. The results reveal that different spacer derivatives resulted in better performance for the photovoltaic (PV) and NLO properties. In particular, ICZS2 and ICZS5 molecules produced excellent performance of the dye-sensitized solar cells (DSSCs) and NLO properties. Based on the theoretical results, the electronic structures and absorption spectra could be used for rational sensitizer design of organic dyes for optoelectronic applications.

Graphical Abstract

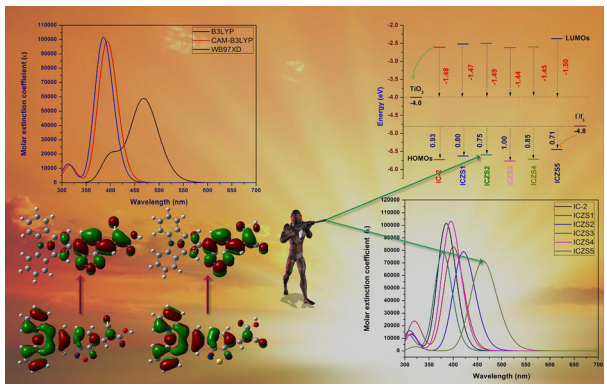

Key words: D-π-A, WB97XD, TD-DFT, NLO, DSSCs

(Received June 18, 2018; accepted December 26, 2018; published online January 8, 2019)

INTRODUCTION

The current energy and environmental crisis has stimulated interest in the development of renewable energy sources. Gratzel and co-workers first developed dye-sensitized solar cells (DSSCs) in 1991. DSSCs have been broadly considered as candidates for renewable-energy systems.[1] In this context, DSSCs have been shown to be an extremely promising methodology for the direct conversion of light into electricity at low cost and with comparatively high efficiency.[2,3] In recent years, a considerable amount of research has been devoted to dye-sensitized solar cells because of their low cost, simplicity of fabrication and high overall power conversion efficiency (PCE).[4] Recently, power conversion efficiency has reached 24.2%, and the same has been confirmed by scientific research reports, but the conventional electricity production process is still noncompetitive,[5] since solar energy is one of most abundant renewable energy resource.

In DSSCs, dye sensitizers are commonly classified into two categories, metal complexes and metal-free organic dyes. Although metal complexes of ruthenium (Ru)-based photosensitizers such as N3 and N719 exhibit impressive light-to-electricity energy conversion efficiency of up to 11%,[6,7] metal-free organic dye sensitizers offer an alternative to Ru complexes due to their low-cost device fabrication, flexibility, environmental friendliness and high molar extinction coefficient. Other major advantages are tunable absorption spectra, easy preparation process, suitable molecular design, unlimited energy resources and PV properties.[8] Recent literature reports indicate achievement of 13.1% PCE using the pure organic sensitizer C281; thus high PCE has been reached with a metal-free organic dye for DSSCs.[9]

Of late, a variety of organic dye sensitizers including triphenylamine (TPA), coumarin, carbazole, phenothiazine (PTZ), indoline and tetrahydroquinoline have been examined and successfully applied in DSSCs.[10–15] For example, *N*,*N*′-dialkylaniline-based (NDI 6) dye used in DSSCs exhibits a PCE of 19.24%, as reported by Kar's group.[16] Among the different DSSCs, the bulk heterojunction model (BHJ) is a successful case.[17–19] Generally, DSSCs contain four major components: a nanocrystalline wide energy bandgap semiconductor photoanode surface (generally TiO_2 or ZnO), a dye sensitizer, redox couple usually containing iodide/triiodide (or) hole transport material, and a counter electrode.

The working principle of DSSCs originates with the photoexcitation process of the dye sensitized under light irradiation. The donor-π-spacer-acceptor (D-π-A) of the dye sensitizers with acceptor moieties is directly bonded to the semiconductor surface of TiO_2. This procedure is called "charge transfer" (CT) or "electron injection".[20] Efficient CT to the conduction band edge (CBE) of a semiconductor is diffused into the substrate to produce electricity. In addition, regeneration of the dyes to the ground state by the redox potential of a liquid electrolyte, electron injection and dye regeneration processes are very important factors in DSSCs performance. Within the past decade, considerable research has been focused on organic dyes containing the structure of D-π-A that can be applied in DSSCs.[21] Most traditional efficient organic dye sensitizers have a long π-conjugated group between donor and acceptor.[22] Successful cases have also been reported using spacer groups in relation to consistent D-π-A structures to enhance the PV cell performance of the DSSCs.[23] In general, organic dyes are necessary for efficient DSSCs possessing broad and extreme absorption in the ultraviolet–visible (UV–Vis) and near-infrared (IR) regions.

In 2014, Luo reported on indolo[3,2,1-jk]carbazole (IC-2) dye-sensitized PV devices exhibiting a high PCE of 3.68%, photovoltage of 0.66 V, and high photocurrent (9.78 mA cm^{-2}) measured under illumination of AM1.5G full sunlight.[24] In addition, IC-2 displays a strong high molar extinction coefficient and useful functionalization that meet important requirements for the development of highly efficient organic dyes for DSSCs.[25,26] In the present work, five spacer groups are introduced based on IC-2 sensitizers, in order to further increase the dye performance of DSSCs. Here, indolocarbazole-3,4-ethylenedioxythiophene, indolocarbazole-benzothiadiazole, indolocarbazole-furan, indolocarbazole-quinoxaline and indolocarbazole-benzoxadiazole (denoted ICZS1, ICZS2, ICZS3, ICZS4 and ICZS5) are used as spacer groups.[27] Additionally, spacer group effects on the D-π-A sensitizer play a vital role in improving the efficiency of DSSCs. Different types of spacer groups have been employed to further increase the optical absorption spectra and PV properties of the organic sensitizers.

The optoelectronic properties of D-π-A designed organic dye molecules have also been studied using density functional theory (DFT) and time-dependent DFT (TD-DFT) approaches. The TD-DFT method is a common choice for studying the first singlet excited state of organic dye molecules.[28] Figure 1 displays the influence of the optoelectronic properties of the DSSCs and NLO based on spacer groups under investigation. In the present work, an approach from previous literature has been followed.[29] Theoretical investigations are helpful for enabling future experimental studies on designed organic dye sensitizers.

QUANTUM CHEMICAL METHODS

DFT optimization and TD-DFT absorption spectra are performed using quantum chemical calculations in Gaussian 09W software.[30] It is well identified that the hybrid functional Becke's three parameter Lee–Yang–Parr (B3LYP) method using a standard basis set 6-31G(*d*) on all atoms have applied DFT calculations.[31,32] The ground-state

geometries are fully optimized using the B3LYP/6-31G(*d*) basis set. The optimized structures with no symmetry constraints are confirmed to be at their true local minima (no imaginary frequency) energy surface. The TD-DFT and selection of different exchange–correlation (XC) functionals was simulated to calculate the UV–Vis absorption spectra. The TD-DFT method was employed in a number of earlier studies to illustrate excited states geometry with CT character.[33] The solvent effect was working with the conductor-like polarizable continuum model (C-PCM) based on ground-state optimization calculations.[34] According to the literature, calculations have been carried out in dichloromethane (DCM) solvent medium.[24]

On the basis of the IC-2 optimized structures, electronic absorption spectra were stimulated using different exchange (XC) and long-range (LC) correlation functionals including B3LYP, Coulomb-attenuating method-B3LYP (CAM-B3LYP)[35] and the Grimme D2 dispersion model (WB97XD).[36] The absolute calculated values for the three functionals are 468 nm, 393 nm and 385 nm. All the calculated values are reported in Table I and shown in Fig. 2. The results show that the absorption spectra from the TD-WB97XD method are in good agreement for the D-π-A system, which contains a spacer unit when compared with IC-2 dye. The calculated error values for the three functionals are 86 nm, 11 nm and 3 nm, compared to the IC-2 dye. From these points of view, the TD-WB97XD method revealed a minimum error of 3 nm. Therefore, the electronic absorption spectra of all organic dyes have been calculated by the TD-WB97XD/6-31G(*d*,*p*) method in this work. The optical absorption wavelength is found using GaussSum.[37]

RESULTS AND DISCUSSION

Screening of π-Spacer Groups

The screening of π-conjugated groups on the D-π-A configuration is an important factor for high-performance DSSC devices in dye molecules. In order to show π-conjugated groups of ICZS1–ICZS5, dye derivatives were systematically designed based on the IC-2 dye. A survey of the literature shows that the use of spacer molecules is a highly efficient approach for organic DSSC applications. In this study, these molecules will affect the indolo[3,2,1-jk]carbazole dye derivatives to enhance optoelectronic properties. The optimized geometric structures of ICZS1–ICZS5 molecules at B3LYP in conjunction with 6-31G(*d*) basis set are shown in supplementary Figure S1, and corresponding input data is provided in the supplementary data file.

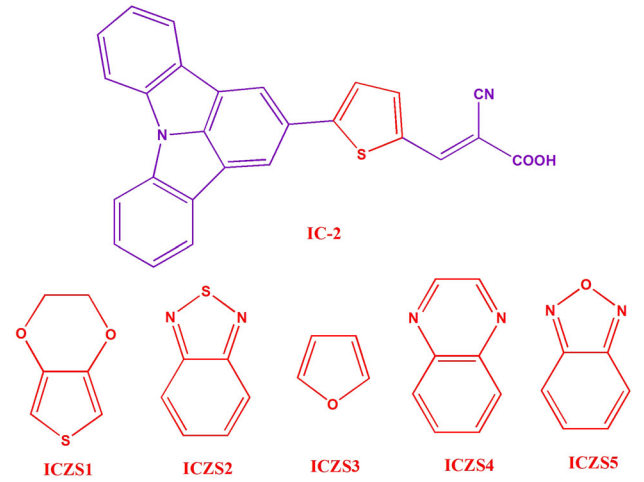

Fig. 1. Sketch map structures of ICZS1–ICZS5 spacer groups.

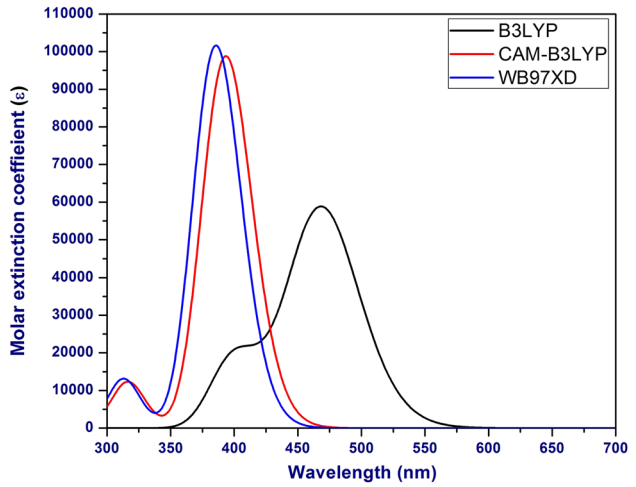

Fig. 2. The computed UV–Vis absorption spectra of the IC-2 molecules using different functional groups with DCM solvent.

Table I. Experimental absorption wavelength, computed vertical excitation energies of the lowest excited state λ_{max} (nm), oscillator strength (*f*) and major orbital configurations of IC-2 dye implemented on different functionals with DCM solvent medium

Methods	λ_{max} (nm)	Oscillator strength (*f*)	Main configuration (%)
B3LYP	468	0.8064	HOMO → LUMO (99)
CAM-B3LYP	393	1.3636	HOMO → LUMO (77)
WB97XD	385	1.4025	HOMO → LUMO (71)
Experiments	382	Taken from Ref. 24	

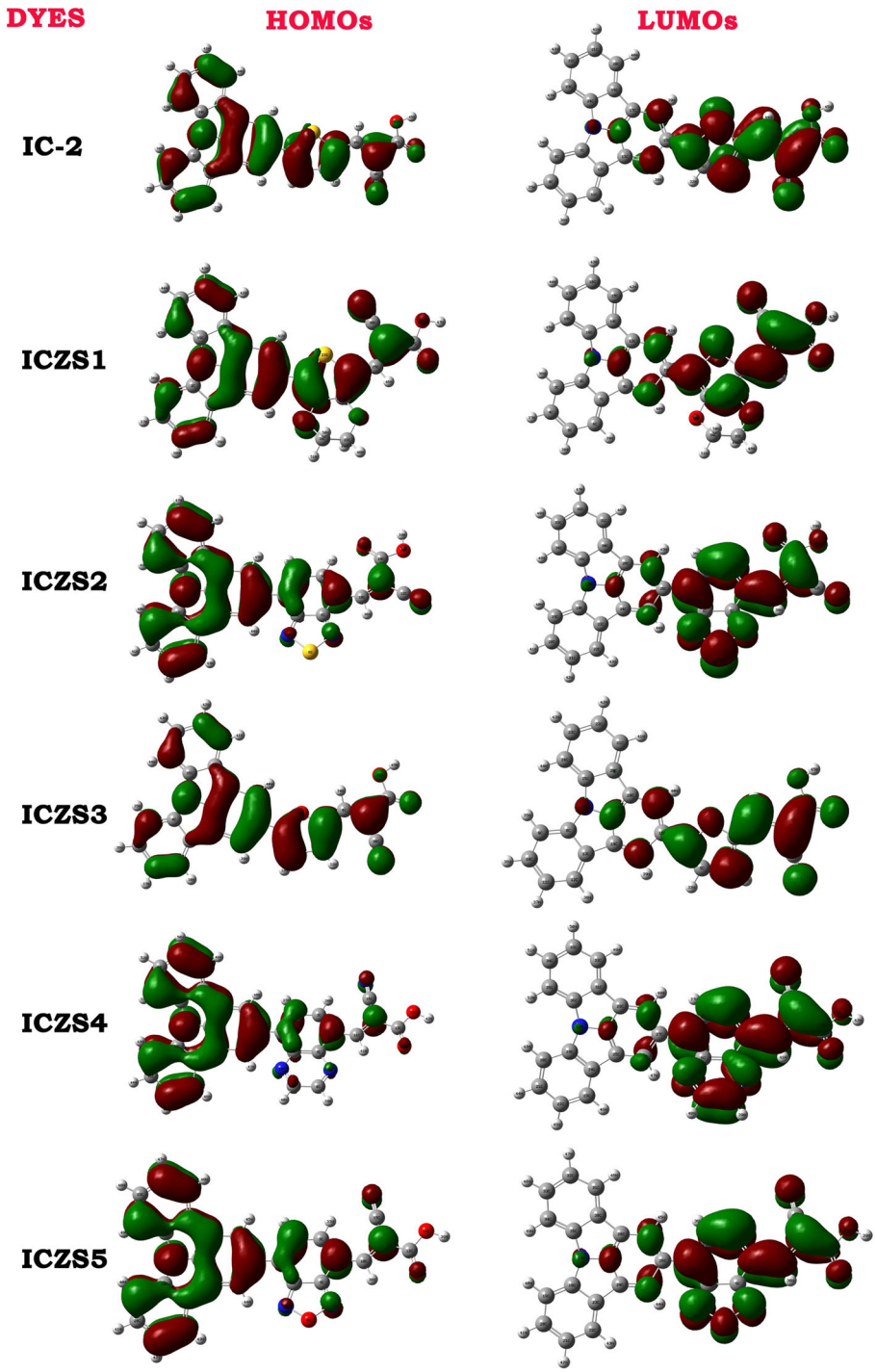

Fig. 3. The frontier molecular orbitals main configuration of HOMO and LUMO levels were calculated at the B3LYP/6-31G(*d*) level of theory.

Electronic Transition and Molecular Orbitals (MOs) Character of Dyes

Figure 3 shows that the molecular orbitals (MOs) and distribution of the highest occupied molecular orbitals (HOMOs) and lowest unoccupied molecular orbitals (LUMOs) of ICZS1–ICZS5 dyes is closely related to the electronic transition characters of dyes.[38] At HOMOs, the electrons are mostly contained in indolocarbazole when dye molecules absorb photons and it will be transferred to cyanoacrylic acid at LUMO levels. Figure 3 displays that HOMOs are mainly localized on the donor with some interaction from the spacer, while the LUMOs are predominantly contained on the acceptor and π-linker segments.

Table II. Molecular orbital energy levels of HOMOs, LUMOs, corresponding energy gap and chemical hardness (η) of the ICZS1–ICZS5 dye molecules performed using the B3LYP/6-31G(*d*) basis set

	B3LYP			
Dyes	**HOMOs (eV)**	**LUMOs (eV)**	**Energy gap (eV)**	**η in (eV)**
IC-2	− 5.73	− 2.61	3.12	1.56
ICZS1	− 5.62	− 2.56	3.06	1.53
ICZS2	− 5.45	− 2.54	2.91	1.45
ICZS3	− 5.83	− 2.69	3.14	1.57
ICZS4	− 5.69	− 2.59	3.10	1.55
ICZS5	− 5.18	− 2.44	2.77	1.38

Therefore, spacers are among the most important factors that affect the performance of dye molecules. The HOMO–LUMO gap between these structures changed when the substituents over spacer groups were modified. The electronic charge transfer (CT) for all dyes is similar, and it is important to note that the electrons can be injected into the semiconductor conduction band edge (CBE) of the TiO_2 surface. The MOs were visualized using Gaussview. MO calculations in HOMOs, LUMOs and energy gaps (E_g) of the ICZS1–ICZS5 dyes are listed in Table II. The HOMO energy levels are in increasing order: ICZS5 < ICZS2 < ICZS1 < ICZS4 < ICZS3, and the LUMOs are in the following order: ICZS5 < ICZS2 < ICZS1 < ICZS4 < ICZS3. A higher LUMO energy level increases the open-circuit photovoltage, leading to a higher PCE of DSSCs.

It is interesting to note that E_g of the dyes are in decreasing order ICZS3 > ICZS4 > ICZS1 > ICZS2 > ICZS5. The more efficient organic dye molecules ICZS1–ICZS5 have smaller E_g as compared to the reference dye IC-2, except the value of ICZS3. In DSSCs, smaller E_g creates more electrons easily at excited states and thus is favorable for absorbing longer light wavelength sides. Therefore, these dyes represent potential energy for providing red-shifted and longer absorption spectra of DSSCs.

Chemical Hardness (η)

Chemical hardness (η) is a suitable parameter for investigating the behavior of chemical systems. The ICZS1–ICZS5 dyes with larger and smaller E_g are known as hard and soft molecules. Chemical η represents the resistance of the dyes to ICT.[39,40]

The chemical η values of the ICZS1–ICZS5 can be calculated using the formula (Eq. 1):

$$\eta = \frac{(E_{\mathrm{HOMO}} - E_{\mathrm{LUMO}})}{2} \qquad (1)$$

All the calculated values of chemical η are listed in Table II. From the table, chemical η decreases in the following order: ICZS3 > ICZS4 > ICZS1 > ICZS2 > ICZS5. Here, ICZS1 and ICZS2 dyes are the same values of 1.55 eV. The stability of a molecule may be determined by the E_g, which means that all dye molecules with low E_g have greater reactivity.

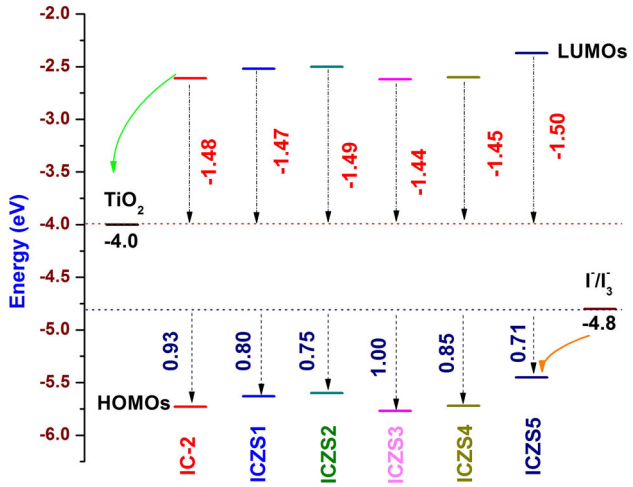

Fig. 4. FMOs of HOMO and LUMO for all dye molecules calculated at the B3LYP/6-31G(*d*) level of theory. The red horizontal dotted line indicates the CBE of TiO_2, and the blue horizontal dotted line indicates the redox electrolyte (Color figure online).

The lowest chemical η further increases charge transport abilities. It is interesting to note that the lowest chemical η values of the ICZS2 and ICZS5 are 1.45 eV and 1.38 eV, respectively. In addition, ICZS2 and ICZS5 molecules are the best candidates for ICT. This demonstrates that ICZS2 and ICZS5 dye molecules can be better suited for both hole and electron transport material compared to IC-2.

Frontier Molecular Orbitals (FMOs)

To understand further, diagrams of the frontier molecular orbitals (FMOs) which determine the charge-separated states of the IC-2 and ICZS1–ICZS5 dyes are shown in Fig. 4. The HOMOs of the dye molecules must lie below the redox electrolyte.[41] The redox potential of the liquid electrolyte is (− 4.8 eV), indicating that it is energetically favorable for ground-state oxidized dye regeneration. Accordingly, all the HOMO energies are below the redox couple. It is noted that this ensures sufficient

Table III. Optical absorption wavelength corresponding excitation energies (λ_{max} in nm and eV), oscillator strength (f in a.u.), orbital transitions (%) and light harvesting efficiency (LHE) of the ICZS1–ICZS5 dyes performed using the TD-WB97XD/6-31G(*d*,*p*) basis set in DCM medium

Dyes	Wavelength		Oscillator strength (*f*)	LHE	Major transitions (%)
	Energy (eV)	λ_{max} (nm)			
IC-2*	3.21	385	1.4025	0.9604	HOMO → LUMO (71%)
ICZS1	3.09	399	1.1440	0.9282	HOMO → LUMO (80%)
ICZS2	2.94	420	0.1026	0.9210	HOMO → LUMO (66%)
ICZS3	3.27	378	1.0856	0.9178	HOMO → LUMO (58%)
ICZS4	3.14	394	1.4251	0.9624	HOMO → LUMO (81%)
ICZS5	2.68	461	0.9881	0.8972	HOMO → LUMO (67%)

*Ref. 24.

driving force for dye regeneration from the redox couple. At the same time, the LUMOs of these dyes must be higher than the CBE of TiO_2 for efficient electron injection, since this will allow the electron injected from the excited states of these dye to reach the CBE of the TiO_2 surface. The CBE of the TiO_2 surface is − 4.0 eV.[42] Figure 4 shows that all the LUMO energies are higher than the CBE of the semiconductor, which implies that the excited states of an electron can be successfully injected into the CBE of TiO_2.

The HOMO and LUMO energy gaps of ICZS1–ICZS5 are smaller than IC-2, which may result in a longer absorption wavelength side and extend into the solar spectrum. It is noted that ICZS2 and ICZS5 have potentially shown good performance when compared to IC-2.

Optical Absorption Properties

First, the absorption spectra of IC-2 dye using three different functionals (B3LYP, CAM-B3LYP and WB97XD) TD-DFT with dichloromethane (DCM) solvent and conductor-like polarizable continuum model (C-PCM) have been investigated and compared with experimental data. The calculated results are listed in Table I. These results obtained with WB97XD functional are closely related to the experimental data (Fig. 2). Secondly, the optical absorption wavelength of the ICZS1–ICZS5 dyes are used in TD-WB97XD functional for calculating. The computed vertical excitation energies corresponding to wavelength, major contribution and oscillator strengths of the dyes in DCM solvent along with available experimental data are listed in Table III and Fig. 5. From Table III, ICZS1–ICZS5 dyes at the calculated values of absorption wavelength were 399 nm, 420 nm, 378 nm, 394 nm and 461 nm. The spacer substituent effects in the ICZS4 dye maximum molar extinction coefficient is (10.32×10^4 M^{-1} cm^{-1}) when compared to IC-2 (10.14×10^4 M^{-1} cm^{-1}) and other dyes. The

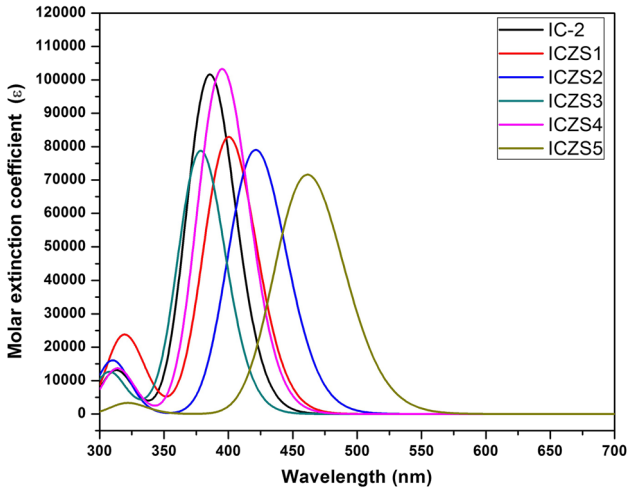

Fig. 5. Simulated absorption spectra of all designed dye molecules ICZS1–ICZS5 and IC-2 were calculated at the TD-WB97XD/6-31G(*d*,*p*) level of theory in DCM solvent.

maximum absorption peaks of the ICZS1, ICZS2, ICZS4, ICZS5 are red-shifted by 14 nm, 35 nm, 9 nm, and 76 nm, and ICZS3 is blue-shifted by 7 nm compared to IC-2.

The light harvesting efficiency (LHE) can be presented using Eq. 2, as follows[43]:

$$LHE = 1 - 10^{-f} \quad (2)$$

Here, f is the oscillator strength (a.u.). The calculated *LHE* values of the ICZS1–ICZS5 dyes are 0.9282 a.u, 0.9210 a.u, 0.9178 a.u, 0.9624 a.u and 0.8972 a.u. The *LHE* of the designed dye molecules must be highly possible for the large photocurrent response for DSSCs. Hence, the *LHE* of ICZS1–ICZS5 dyes exceed the potential to give a more or less similar photocurrent. In particular, the *LHE* of ICZS4 dye is larger than that of IC-2.

Generally, dye molecules with low E_g can create more electrons at the UV–Vis and near-infrared regions and increase the efficiency of DSSCs. Therefore, the presence of added spacer groups kindly enhances the ICZS1, ICZS2, ICZS4 and ICZS5 dyes are red-shifted in the absorption spectra, which may be favorable for enhancing efficient in DSSCs.

Non-linear Optical (NLO) Properties

Over the past decade, various research teams have studied NLO response using organic dye molecules.[29,44] A smaller E_g leads to higher NLO property response. The NLO properties characterize the response of a system to an applied electric field. In this study, the NLO properties using spacers with ICZS1–ICZS5 dyes are calculated. The NLO properties of the dye molecules are calculated by the static dipole moment (μ), polarizability (α), static polarizability ($\Delta\alpha$) and first (β_0) order hyperpolarizability.

The μ, α, $\Delta\alpha$ and β_0 are expressed as follows:

$$\mu = \sqrt{\mu_x^2 + \mu_y^2 + \mu_z^2} \tag{3}$$

$$\alpha_{\text{tot}} = \frac{1}{3}\left[\alpha_{xx} + \alpha_{yy} + \alpha_{zz}\right] \tag{4}$$

$$\Delta\alpha = \frac{1}{\sqrt{2}}\left[\left(\alpha_{xx} + \alpha_{yy}\right)^2 + \left(\alpha_{zz} + \alpha_{xx}\right)^2 + 6\alpha_{xx}^2\right] \tag{5}$$

$$\beta_0 = \left[\left(\beta_{xxx} + \beta_{xyy} + \beta_{xzz}\right)^2 + \left(\beta_{xxy} + \beta_{yyy} + \beta_{yzz}\right)^2 + \left(\beta_{xxz} + \beta_{zyy} + \beta_{zzz}\right)^2\right]^{\frac{1}{2}} \tag{6}$$

Here, $\mu_x^2, \mu_y^2, \mu_z^2$ dipole tensor components and α_{xx}, α_{yy} and α_{zz} polarizability tensor components, $\beta_{xxz}, \beta_{zyy}, \beta_{zzz}, \beta_{xxx}, \beta_{xyy}, \beta_{xzz}, \beta_{xxy}, \beta_{yyy}$ and β_{yzz} magnitude of the first hyperpolarizability tensor components. These constraints contribute to the nonlinearity of the designed dye molecules.

The calculated values of μ, α, $\Delta\alpha$, β_0 at the ground state for the ICZS1–ICZS5 and IC-2 dyes are listed in supplementary Table SI. The μ is an essential factor that provides data about the electronic charge spreading in the molecules. The results for μ showed that the larger values of the ICZS2 dye are 9.40 Debye and 10.98 Debye in gas and solvent phases compared to IC-2. Among the five dyes, ICZS2 exhibits the best performance of NLO activity.

From the table α values of ICZS2 (207 a.u.), ICZS4 (195 a.u.) and ICZS5 (195 a.u.) are higher than the other dyes when compare to IC-2 (186 a.u.). The maximum value of the ICZS2 molecule is 3.074×10^{-23} e.s.u. compared with IC-2 is 2.764×10^{-23} e.s.u. The highest value of β_0, which is a measurement of the NLO activity of the molecular system and is closely associated with ICT. Consequently, ICZS2 and ICZS5 molecules are greater than the 6.511×10^{-30} e.s.u. and 6.279×10^{-30} e.s.u. compared to reference dye is 5.858×10^{-30} e.s.u. The highest α and β_0 exhibit good sensitizing properties upon photoexcitation. A quantum chemical study has been used to understand the relationship between the electronic structure and its NLO response. A higher value of β_0 specifies significant active NLO performance, and the current results show that the ICZS2 and ICZS5 dyes were particularly suited for use in NLO applications.

Photovoltaic Properties

Power Conversion Efficiency

The power conversion efficiency (P_{CE}) of the DSSCs was calculated according to Eq. 7,[45] as follows:

$$P_{CE} = 1/P_{INC}(V_{OC}J_{SC}FF) \tag{7}$$

where P_{INC} denoted as incident power density, V_{OC} is the open-circuit photovoltage, and FF is the fill factor. The maximum V_{OC} values of the DSSCs are mainly determined by the LUMOs and CBE of the Fermi level.

The theoretical values of eV_{OC} have been calculated from following Eq. 8[46]:

$$eV_{OC} = E_{LUMO} - E_{CB}^{TiO_2} \tag{8}$$

The theoretical values of the eV_{OC} for the studied ICZS1–ICZS5 molecules range from 1.31 eV to 1.56 eV. These values are sufficient for a potential efficient electron injection process. In addition, higher values of LUMOs will generate larger eV_{OC}, which contributes to the conversion efficiency of the organic solar cells. It is shown that the ICZS2 and ICZS5 have larger eV_{OC} values compared to IC-2 and other dyes. The results show that the substitution effects of ICZS1, ICZS2, ICZS4 and ICZS5 dyes have enhanced eV_{OC}. In particular, ICZS2 and ICZS5 dyes show a higher eV_{OC}, which indicates the outstanding performance of dyes.

Therefore, all the designed molecules can be used for the dye-sensitized cells, because the electron injection process from the excited state molecules to the CBE of the TiO_2 has been successful. In addition, it is favorable for subsequent dye regeneration in an organic solar cell.

Electron Injection and Dye Regeneration

The electronic properties of the dye molecules in the first excited state are a significant factor in the performance of DSSCs. The J_{SC} main influencing parameters of the electron injection (ΔG_{inject}), oxidation potential energy (E^{dye^*}) and dye regeneration

Table IV. The calculated redox potential of the ground state (E^{dye} in eV), vertical excitation energy (λ_{max} in eV), electron injection (ΔG_{inject} in eV), dye regeneration (ΔG_{reg} in eV) and open circuit photovoltage (eV_{OC}) of the studied dye molecules implemented on the TD-WB97XD/6-31G(*d*,*p*) basis set in DCM solvent medium

	In (eV)					
Dyes	E^{dye}	λ_{max}	E^{dye^*}	ΔG_{inject}	ΔG_{reg}	eV_{OC}
IC-2	5.73	3.21	2.52	− 1.48	0.93	1.39
ICZS1	5.62	3.09	2.53	− 1.47	0.80	1.44
ICZS2	5.45	2.94	2.51	− 1.49	0.75	1.46
ICZS3	5.83	3.27	2.56	− 1.44	1.00	1.31
ICZS4	5.69	3.14	2.55	− 1.45	0.85	1.41
ICZS5	5.18	2.68	2.83	− 1.50	0.71	1.56

(ΔG_{reg}) for the excited state in ICZS1–ICZS5 molecules were calculated using formulas as defined in a previous study,[47] and the values are listed in Table IV. Theoretically proposed that the ΔG_{inject} from the dye molecules in the unrelaxed excited state to the CBE of the semiconductor.[48] According to Islam's theory, when $\Delta G_{inject} > 0.2$ eV.[49] Consequently, the absolute calculated values of ICZS1–ICZS5 dyes are much greater than 0.2 eV. From Table IV, it is obvious that all the ΔG_{inject} calculated values are negative, which means that the excited state of the dye lies above the CBE of the TiO_2. ICZS1–ICZS5 have an energy difference of − 1.44 eV to − 1.50 eV between the excited state molecules and CBE of TiO_2. Hence, it is large enough to guarantee efficient ΔG_{inject}, except the value of ICZS3. On the other hand, too large a value of ΔG_{inject} might include energy redundancy, which could result from a smaller V_{OC} and large thermalization losses.[50,51]

In order to attain faster electron transfer, it is essential to reduce regeneration.[52] The calculated ΔG_{reg} values of all the dye molecules are listed in Table IV. The ΔG_{reg} of ICZS1, ICZS2, ICZS4 and ICZS5 are lower than the IC-2 (0.93 eV), indicating the high PCE of the DSSCs. Because of the significance of the data, the higher ΔG_{inject},eV_{OC} and the broader absorption spectra, as well as small E_g and ΔG_{reg}, high conversion efficiency was achieved. Hence, DSSCs in ICZS2 and ICZS5 dyes are superior candidates to other dyes, due to these favorable computed results. In summary, indolocarbazole dye derivatives can be systematically modified through various π-spacers for DSSC application.

CONCLUSION

In summary, the optoelectronic properties of indolocarbazole (IC-2) based ICZS1–ICZS5 spacer molecules were systematically investigated by DFT and TD-DFT in detail. The spacer effect of the electronic structures, absorption wavelength and NLO properties were detailed as discussed. The computed absorption spectra using the TD-DFT method including the WB97XD functional show good agreement with the IC-2. The calculated results show that the LUMOs energy of ICZS2 and ICZS5 mainly delocalized on the spacer groups which are favorable for TiO_2. This is possible due to the effectiveness of the molecules for electron injection into the CBE of TiO_2. Additionally, their HOMO energy is in good agreement with that of dye regeneration, making them suitable for use in DSSCs. The UV–Vis absorption spectra of ICZS2 and ICZS5 showed better red shifts compared with IC-2. In fact, ICZS2 and ICZS5 molecules produced higher open-circuit voltage in DSSC devices. The calculated results also show that dipole moment, polarizability and first hyperpolarizability values at ICZS2 and ICZS5 molecules have a better NLO response. The results of this study may be useful for the development of sensitizers with desirable optical and electronic properties in order to achieve DSSCs with higher efficiency.

ACKNOWLEDGMENTS

The authors are thankful to the learned referees for their useful and critical comments, which improved the quality of the manuscript.

CONFLICT OF INTEREST

The authors declare that there is no conflict of interest.

ELECTRONIC SUPPLEMENTARY MATERIAL

The online version of this article (https://doi.org/10.1007/s11664-018-06912-x) contains supplementary material, which is available to authorized users.

REFERENCES

1. B. O'Regan and M. Gratzel, *Nature* 353, 737 (1991).
2. Y. Wu and W. Zhu, *Chem. Soc. Rev.* 42, 2039 (2013).
3. C.P. Lee, C.Y. Chou, C.Y. Chen, M.H. Yeh, L.Y. Lin, R. Vittal, C.G. Wu, and K.C. Ho, *J. Power Sources* 246, 1 (2014).

4. S. Zhang, X. Yang, Y. Numata, and L. Han, *Energy Environ. Sci.* 6, 1443 (2013).
5. M.A. Green, K. Emery, Y. Hishikawa, and W. Warta, *Prog. Photovolt.* 18, 144 (2010).
6. M.K. Nazeeruddin, F.D. Angelis, S. Fantacci, A. Selloni, G. Viscardi, P. Liska, S. Ito, B. Takeru, and M. Grätzel, *J. Am. Chem. Soc.* 127, 16835 (2005).
7. C.-Y. Chen, M.K. Wang, J.-Y. Li, N. Pootrakulchote, L. Alibabaei, C.H. Ngoc-le, J.D. Decoppet, J.H. Tsai, C. Grätzel, C.G. Wu, and S.M. Zakeeruddin, *ACS Nano* 3, 3103 (2009).
8. T. Kitamura, M. Ikeda, K. Shigaki, T. Inoue, N.A. Anderson, X. Ai, T.Q. Lian, and S. Yanagida, *Chem. Mater.* 16, 1806 (2004).
9. Z. Yao, H. Wu, Y. Li, J.T. Wang, J. Zhang, M. Zhang, Y.C. Guo, and P. Wang, *Energy Environ. Sci.* 8, 3192 (2015).
10. F. Wu, L.T.L. Lee, J. Liu, S. Zhao, T. Chen, M. Wang, and L. Zhu, *Synth. Met.* 205, 70 (2015).
11. R. Sánchez-de-Armas, M.A. San, J. Miguel, J. Oviedo, and J.F. Sanz, *Phys. Chem. Chem. Phys.* 14, 225 (2012).
12. Z.-S. Wang, N. Koumura, Y. Cui, M. Takahashi, H. Sekiguchi, A. Mori, T. Kubo, A. Furube, and K. Hara, *Chem. Mater.* 20, 3993 (2008).
13. Z. Wan, C. Jia, Y. Duan, L. Zhou, J. Zhang, Y. Lin, and Y. Shi, *RSC Adv.* 2, 4507 (2012).
14. J. Sobus, J. Karolczak, D. Komar, J.A. Anta, and M. Ziółek, *Dyes Pigm.* 113, 692 (2015).
15. Y. Hao, X. Yang, J. Cong, A. Hagfeldt, and L. Sun, *Tetrahedron* 68, 552 (2012).
16. S. Kar, J.K. Roy, and J. Leszczynski, *NPJ Comput. Mater.* 3, 22 (2017).
17. G. Yu, J. Gao, J.C. Hummelen, F. Wudl, and A. Heeger, *Science* 270, 1789 (1995).
18. Y.J. Cheng, S.H. Yang, and C.S. Hsu, *Chem. Rev.* 109, 5868 (2009).
19. T.-Y. Chu, J. Lu, S. Beaupré, Y. Zhang, J.-R. Pouliot, S. Wakim, J. Zhou, M. Leclerc, Z. Li, J. Ding, and Y. Tao, *J. Am. Chem. Soc.* 133, 4250 (2011).
20. D. Rocca, R. Gebauer, F. De Angelis, M.K. Nazeeruddin, and S. Baroni, *Chem. Phys. Lett.* 475, 49 (2009).
21. A. Arunkumar and P.M. Anbarasan, *J. Comput. Electron.* 17, 1410 (2018).
22. S. Ahmad, E. Guillen, L. Kavan, M. Grätzel, and M.K. Nazeeruddin, *Energy Environ. Sci.* 6, 3439 (2013).
23. X. Ren, S. Jiang, M. Cha, G. Zhou, and Z.-S. Wang, *Chem. Mater.* 24, 3493 (2012).
24. C. Luo, W. Bi, S. Deng, J. Zhang, S. Chen, B. Li, Q. Liu, H. Peng, and J. Chu, *J. Phys. Chem. C* 118, 14211 (2014).
25. X.H. Zhang, Z.S. Wang, Y. Cui, N. Koumura, A. Furube, and K. Hara, *J. Phys. Chem. C* 113, 13409 (2009).
26. S. Cai, G. Tian, X. Li, J. Su, and H.J. Tian, *J. Mater. Chem. A* 1, 11295 (2013).
27. X. Zhang, M. Grätzel, and J. Hua, *Front. Optoelectron.* 9, 3 (2016).
28. C.A. Guido, S. Knecht, J. Kongsted, and B. Mennucci, *J. Chem. Theory Comput.* 9, 2209 (2013).
29. A. Arunkumar and P.M. Anbarasan, *Struct. Chem.* 29, 967 (2018).
30. M.J. Frisch, G.W. Trucks, H.B. Schlegel, G.E. Scuseria, M.A. Robb, J.R. Cheeseman, G. Scalmani, V. Barone, B. Mennucci, G.A. Petersson, H. Nakatsuji, M. Caricato, X. Li, H.P. Hratchian, A.F. Izmaylov, J. Bloino, G. Zheng, J.L. Sonnenberg, M. Hada, M. Ehara, K. Toyota, R. Fukuda, J. Hasegawa, M. Ishida, T. Nakajima, Y. Honda, O. Kitao, H. Nakai, T. Vreven Jr., J.A. Montgomery, J.E. Peralta, F. Ogliaro, M.J. Bearpark, J. Heyd, E.N. Brothers, K.N. Kudin, V.N. Staroverov, R. Kobayashi, J. Normand, K. Raghavachari, A.P. Rendell, J.C. Burant, S.S. Iyengar, J. Tomasi, M. Cossi, N. Rega, N.J. Millam, M. Klene, J.E. Knox, J.B. Cross, V. Bakken, C. Adamo, J. Jaramillo, R. Gomperts, R.E. Stratmann, O. Yazyev, A.J. Austin, R. Cammi, C. Pomelli, J.W. Ochterski, R.L. Martin, K. Morokuma, V.G. Zakrzewski, G.A. Voth, P. Salvador, J.J. Dannenberg, S. Dapprich, A.D. Daniels, Ö. Farkas, J.B. Foresman, J.V. Ortiz, J. Cioslowski, and D.J. Fox, *Gaussian 09* (Wallingford: Gaussian Inc., 2009).
31. A.D. Becke, *J. Chem. Phys.* 98, 5648 (1993).
32. C. Lee, W. Yang, and R.G. Parr, *Phys. Rev. B* 37, 785 (1988).
33. F.D. Angelis, S. Fantacci, and A. Selloni, *Nanotechnology* 19, 424002 (2008).
34. J. Tomasi, B. Mennucci, and R. Cammi, *Chem. Rev.* 105, 2999 (2005).
35. T. Yanai, D.P. Tew, and N.C. Handy, *Chem. Phys. Lett.* 393, 51 (2004).
36. Y.-S. Lin, G.-D. Li, S.-P. Mao, and J.-D. Chai, *J. Chem. Theory Comput.* 9, 263 (2012).
37. N.M. O'Boyle, A.L. Tenderholt, and K.M. Langner, *J. Comput. Chem.* 29, 839 (2008).
38. Y. Zhao and W.Z. Liang, *Chem. Soc. Rev.* 41, 1075 (2012).
39. J.I. Nishida, T. Masuko, Y. Cui, K. Hara, H. Shibuya, M. Ihara, T. Hosoyama, R. Goto, S. Mori, and Y. Yamashita, *J. Phys. Chem. C* 114, 17920 (2010).
40. R.G. Pearson, *Proc. Natl. Acad. Sci.* 83, 8440 (1986).
41. M. Liang and J. Chen, *Chem. Soc. Rev.* 42, 3453 (2013).
42. D.O. Scanlon, C.W. Dunnill, J. Buckeridge, S.A. Shevlin, A.J. Logsdail, S.M. Woodley, C.R.A. Catlon, M.J. Powell, R.G. Palgrave, I.P. Parkin, G.W. Watson, T.W. Keal, P. Sherwood, A. Walsh, and A.A. Sokol, *Nat. Mater.* 12, 798 (2013).
43. Z.L. Zhang, L.Y. Zou, A.M. Ren, Y.F. Liu, J.K. Feng, and C.C. Sun, *Dyes Pigm.* 96, 349 (2013).
44. P. Senthilkumar, C. Nithya, and P.M. Anbarasan, *Spectrochim. Acta A Mol. Biomol. Spectrosc.* 122, 15 (2014).
45. A. Gadisa, M. Svensson, M.R. Andersson, and O. Inganas, *Appl. Phys. Lett.* 84, 1609 (2004).
46. W. Sang-aroon, S. Saekow, and V. Amornkitbamrung, *J. Photochem. Photobiol. A* 236, 35 (2012).
47. A. Fitri, A.T. Benjelloun, M. Benzakour, M. Mcharfi, M. Hamidi, and M. Bouachrine, *Spectrochim. Acta Part A Mol. Biomol. Spectrosc.* 132, 232 (2014).
48. A. Arunkumar, M. Prakasam, and P.M. Anbarasan, *Bull. Mater. Sci.* 40, 1389 (2017).
49. A. Islam, H. Sugihara, and H. Arakawa, *J. Photochem. Photobiol. A* 158, 131 (2003).
50. M. Nakano, H. Fujita, M. Takahata, and K. Yamaguchi, *J. Am. Chem. Soc.* 124, 9648 (2002).
51. V.M. Geskin, C. Lambert, and J.L. Bredas, *J. Am. Chem. Soc.* 125, 15651 (2003).
52. M. Li, L. Kou, L. Diao, Q. Zhang, Z. Li, Q. Wu, W. Lu, D. Pan, and Z. Wei, *J. Phys. Chem. C* 119, 9782 (2015).